Vortices in fermion droplets with repulsive dipole-dipole interactions

G. Eriksson,[1] J. C. Cremon,[1] M. Manninen,[2] and S. M. Reimann[1]

[1]*Mathematical Physics, LTH, Lund University, SE-22100 Lund, Sweden*
[2]*Nanoscience Center, Department of Physics, University of Jyväskylä, FI-40014 Jyväskylä, Finland*

Vortices are found in a fermion system with *repulsive* dipole-dipole interactions, trapped by a rotating quasi-two-dimensional harmonic oscillator potential. Such systems have much in common with electrons in quantum dots, where rotation is induced via an external magnetic field. In contrast to the Coulomb interactions between electrons, the (externally tunable) anisotropy of the dipole-dipole interaction breaks the rotational symmetry of the Hamiltonian. This may cause the otherwise rotationally symmetric exact wave function to reveal its internal structure more directly.

PACS number(s): 67.85.−d, 03.75.Lm, 05.30.Fk

I. INTRODUCTION

Rotating quantum fluids have been studied for a long time, with the interest being spurred by their many fascinating properties. A prominent example are superfluids such as liquid helium [1]. When set rotating in a bucket, for sufficiently large rotation, the quantum liquid becomes penetrated by quantized vortices, forming the well-known Abrikosov lattice.

After the early prediction of Bose and Einstein in the 1920s [2], it was not until 1995 that the condensation of a gas of bosonic atoms into a single coherent quantum state could be achieved [3]. Stirring the condensate with lasers or rotating the trap that confines the dilute atom gas, vortices similar to those in ^{4}He [4,5] were observed [6,7] (see also the review by Fetter [8]). Similar states have been realized also for trapped fermionic atoms with attractive interactions where pairing or molecule formation can occur (see the reviews [9,10]).

Apart from their presence in systems with bosons, vortices have also been predicted to occur in fermion systems with purely *repulsive* interactions, such as quantum dots—small man-made electronic systems that can be created in a semiconductor heterostructure [11], where the rotation can be induced with an external magnetic field. For small numbers of confined electrons, it was shown that these fermionic quantum Hall droplets form vortices in a very similar way to repulsive bosons set rotating in the trap [12–14]. This analogy may question the commonly accepted view that vortices and vortex arrays may be taken as a criterion of superfluid properties [15]. Experimentally, however, vortices in quantum dots are difficult to detect: As the electrons are inside a semiconductor crystal, probing their properties must typically be done by indirect methods. Examples are electron transport or magnetization measurements [15,16]. These are, however, strongly hindered by the restricted resolution in the conductance spectra, as well as unavoidable sample imperfections.

Here, ultracold atomic gases may be the better choice, as they typically are very clean, and remarkable characterization techniques have been demonstrated. For example, it is possible to directly image the atomic cloud after expansion. Atomic quantum gases usually confine millions of atoms, bringing system sizes close to the thermodynamic limit. Serwane *et al.* [17], however, showed recently that the confinement of about a dozen of cold fermionic atoms can be reached experimentally.

The electrons in a quantum dot interact via long-range repulsive Coulomb forces. An alternative is provided by atoms or molecules with (either electric or magnetic) dipole-dipole interactions providing a long-range coupling between the particles. (There has recently been much interest in such dipolar systems; see, for example, Refs. [18–23] and [24,25] for reviews.) In contrast, the very short-ranged van der Waals interaction has a limited effect on spin-polarized fermions due to the Pauli exclusion principle and might not give a similar response to rotation as long-range interactions.

In this paper, we show that vortices and vortex clusters occur in a (spin-polarized) fermion droplet with strictly repulsive dipole-dipole interactions, in analogy to vortices in a quantum dot. While in quantum dots the vortex lattice still awaits experimental detection, we suggest that dipolar fermionic atoms with repulsive interactions may indeed show a vortex lattice similar to analogous systems with bosons.

II. MODEL

As a simple model (that resembles electrons in a quantum dot) we consider a few (spin-polarized) fermions confined in a rotationally symmetric two-dimensional harmonic oscillator in the xy plane, with oscillator frequency ω_0. We assume that the particles are confined in the z direction with a tight harmonic oscillator, so that the total trapping potential is $V_{\text{trap}}(x,y,z) = \frac{1}{2}m\omega_0^2(x^2 + y^2) + \frac{1}{2}m\omega_z^2 z^2$. The oscillator length l_z is here set to be $1/100$ of that in the plane, so that the particles occupy the lowest orbital in this direction. (In the following, we work in dimensionless oscillator units; that is, lengths are given in units of $l_0 = \sqrt{\hbar/(m\omega_0)}$, energies in $\hbar\omega_0$, and frequencies in ω_0.) The rotation is induced by adding a term $-\Omega\hat{L}$ to the Hamiltonian, where Ω is the rotational (angular) frequency of the rotating trap and $\hat{L}$ is the (z projection) of the angular momentum operator.

For the interaction between the fermions we assume that their dipole moments are aligned by an external field. This makes it possible to control the effective anisotropy of the interaction, breaking the rotational symmetry in the system. A few other theoretical studies considered very similar setups [26–28]. Here, however, the focus is on the vortex structure.

For two particles with dipole moments, a general expression for their interaction energy is given in Ref. [24]. In the present

system, we assume the dipole moments to be aligned to an axis lying in the xz plane, such that this axis forms an angle Θ with the xy plane where the particles are effectively confined by the harmonic trapping. For two-point dipoles confined to the xy plane, the interaction is attractive for $\Theta < \arccos \frac{1}{\sqrt{3}} \approx 54.7°$. To avoid the possibility that the system collapses in the case of attractive interactions, we restrict the tilting to the interval $54.7° \lesssim \Theta \leqslant 90°$, where the interaction is repulsive. The coordinate system used here is corotating with the trap (at frequency Ω), meaning that the dipole axis is rotating in the laboratory frame. The in-plane interaction between the particles is obtained by analytically integrating their motion along the z direction, where the particles are assumed to be in the lowest oscillator state. This results in the interaction potential

$$
\begin{aligned}
V_{2D}(r,\phi) = \frac{D^2}{2\sqrt{2}} \frac{e^{\xi/2}}{(l_z/l_0)^3} & \{(2+2\xi)K_0(\xi/2) - 2\xi K_1(\xi/2) \\
& + \cos^2\Theta[-(3+2\xi)K_0(\xi/2) + (1+2\xi)K_1(\xi/2)] \\
& + 2\cos^2\Theta\cos^2\phi[-\xi K_0(\xi/2) \\
& + (\xi-1)K_1(\xi/2)]\},
\end{aligned}
\tag{1}
$$

where K_0 and K_1 are irregular modified Bessel functions, and $\xi = r^2/[2(l_z/l_0)^2]$. The prefactor D is here dimensionless; for an electrical dipole it corresponds to $D = \frac{d}{\sqrt{4\pi\epsilon_0}} \frac{\sqrt{m}}{\hbar\sqrt{l_0}}$, where d is the dipole moment, and similarly for a magnetic dipole [29]. The expression in Eq. (1) (or special cases of it) is given, for example, in Refs. [27,29–32]. Only for $\Theta = 90°$ does the interaction have rotational symmetry. In this limit, it is qualitatively similar to the electrostatic Coulomb interaction but more short ranged. For other angles, the two-body term is spatially anisotropic (cf. Fig. 1 in Ref. [29]).

The ratio l_z/l_0 enters above, and as it is typically much smaller than one, at first sight it gives a very large interaction strength. However, this ratio also enters elsewhere in the expression so that its final behavior is more subtle. It turns out that for long ranges, Eq. (1) is practically independent of l_z/l_0 and proportional to D^2/r^3. (*Long range* here corresponds
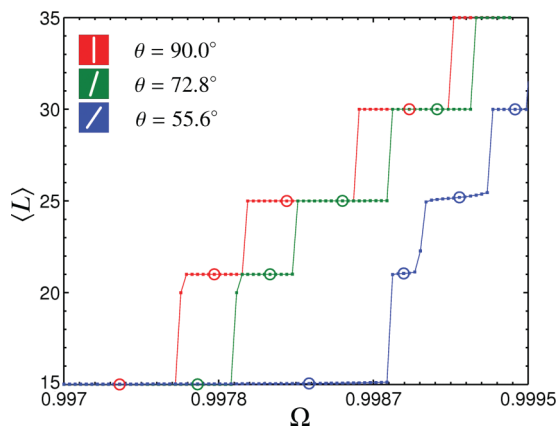

FIG. 1. (Color online) Expectation value of the angular momentum L of the ground state, as a function of the rotational frequency Ω, for three different tilt angles of the dipoles. The system consists of $N = 6$ (spin-polarized) fermions with dipole-dipole interactions. As Ω increases, the angular momentum changes discontinuously, and vortices penetrate the quantum system. The states marked with circles are the ones shown in the following figures.

to $r \gg l_z/l_0$.) At short range the coefficient $\frac{D^2}{(l_z/l_0)^3}$ does have an impact on the value of the interaction potential, but in this study we only consider spin-polarized fermions, for which the Pauli exclusion principle eliminates the effect of the interaction at short ranges.

The many-body Hamiltonian

$$
H = \sum_{i=1}^{N} \left(\frac{1}{2}\mathbf{p}_i^2 + \frac{1}{2}\mathbf{r}_i^2 \right) + \frac{1}{2}\sum_{i\neq j}^{N} V_{2D}(\mathbf{r}_i - \mathbf{r}_j) - \Omega\hat{L} \tag{2}
$$

is then diagonalized numerically, applying the configuration interaction method (also called "exact" diagonalization). The commonly used lowest Landau level approximation [15] allows us to restrict the Hilbert space to a basis of Slater determinants constructed with the single-particle orbitals $\psi_{n=0,m\geqslant 0}(r,\varphi) = \frac{1}{\sqrt{m!\pi}} r^m e^{im\varphi} e^{-r^2/2}$ of the two-dimensional harmonic oscillator. This is a reasonable approximation in the limit when the rotational frequency Ω is close to, but smaller than, the trapping frequency ω_0 and the interaction is weak. We set the interaction strength $D = 0.1$ to assure that the interaction energy is smaller than the Landau level spacing, which is of order $\hbar\omega_0$. In the calculations, sufficiently large m values are included so that the resulting energies are unaffected by this cutoff.

III. RESULTS

Characteristic for the response of the system to a monotonously increasing trap rotation Ω is the change in angular momentum $L(\Omega)$, obtained by minimizing the total energy in the rotating frame of reference as a function of Ω. For a superfluid, after the onset of trap rotation, the system first remains at rest, $L = 0$, until a critical frequency is reached beyond which vortices begin to penetrate the cloud. As Ω further increases, the angular momentum changes discontinuously to higher values as additional vortices appear. For a rotating Bose-Einstein condensate, this sequential appearance of vortices was predicted by applying the mean-field Gross-Pitaevskii approach [4,5] and later also observed experimentally [6,7].

For electrons in quantum dots, the rotation may be induced by an applied magnetic field. In the limit of slow rotation, vortices and vortex clusters occur even though there is no condensation of bosons present. (For a more detailed discussion, see, e.g., Refs. [13,15].)

Turning now to fermions with repulsive dipole-dipole interactions, for small particle numbers and relatively slow rotation considered here, we find that indeed the system shows a similar vortex pattern.

When we solve the many-body Hamiltonian by direct diagonalization, the numerical effort grows considerably with particle number. Because of the anisotropic dipole-dipole interaction, angular momentum is not a good quantum number, which poses an additional limitation to the system sizes that are numerically accessible. For this reason we here limit the study to six particles confined in the harmonic trap, making use of the lowest Landau level (LLL) appropriate for weak interactions.

In the case of noninteracting bosons, the many-particle ground state is the permanent $|N0000\ldots\rangle$ with macroscopic occupancy of the $m = 0$ orbital in the LLL basis. For

spinless fermions, however, the Pauli principle demands single occupancy of the orbitals, leading to the so-called maximum density droplet $|111111000\ldots\rangle$. This state represents the finite-size analog to the Laughlin state for the integer quantum Hall effect and is the fermionic equivalent to the condensate permanent. The lowest possible angular momentum of this Slater determinant is $L_{\mathrm{MDD}} = N(N-1)/2$.

The response of the system with $N = 6$ dipolar fermions to the increasing trap rotation Ω is shown in Fig. 1 for different values of the dipolar tilt angle θ, where the interactions are in the repulsive regime. (Note that since L is not a good quantum number, we instead calculate the corresponding expectation value that can be noninteger.) Qualitatively, the resulting picture is very similar as for trapped bosons or electrons in quantum dots.

A. Isotropic interaction

Let us first consider the case of aligned dipoles with $\theta = 90.0°$. At moderate rotation, the cloud remains at rest relative to the angular momentum of the MDD (here, $L_{\mathrm{MDD}} = 15$), until a critical frequency is reached, where the first step in $L(\Omega)$ occurs, and the system acquires angular momentum beyond the MDD value. At this frequency a vortex is formed at the center of the cloud (see discussion below). With increasing rotation, further steps occur that are associated with the entry of additional vortices. The tilt angle of the dipole axis is found to have little effect on $L(\Omega)$: The jumps are mainly shifted to higher values of Ω as the angle is lowered. This can be understood by noting that the tilt of the dipole angle not only makes the interactions anisotropic but also effectively lowers their strength.

The single-particle density distribution, however, defined as $\rho(\mathbf{r}) = \langle\Psi|\hat{\Psi}^\dagger(\mathbf{r})\hat{\Psi}(\mathbf{r})|\Psi\rangle$, can be strongly affected by the tilt, as shown in Fig. 2. If the dipoles are aligned perpendicularly to the plane of motion ($\Theta = 90°$), the Hamiltonian has rotational symmetry. Hence, the density of the associated eigenstates should also be azimuthally symmetric. This makes it impossible to identify vortex clusters beyond the simple unit vortex (that has azimuthal symmetry). Internally, for the two-vortex solution, the two single vortices appear as a pair with twofold symmetry, while the three-vortex solution locates the vortices at the corners of an equilateral triangle. However, if the Hamiltonian has rotational symmetry these structures cannot be visible in the single-particle density. (The pair-correlated density, though, can reveal them, as discussed later in the text.) This is in contrast with wave functions obtained from mean-field approximations such as the Hartree-Fock or the Gross-Pitaevskii equations, where broken-symmetry solutions are possible.

B. Anisotropic interaction

When the dipole axis is tilted, the rotational symmetry is broken. Though some states are not significantly affected by the tilt—for example, the state with a single vortex at the center—with increasing Ω, the state with $\langle L\rangle \approx 25$ now shows two clear off-center minima in its density (see Fig. 2). The overlap of this state at $\Theta = 55.6°$ with that at $\Theta = 90°$ is 93.1%, showing that the internal structure of the quantum state is largely unchanged despite the seemingly different densities.
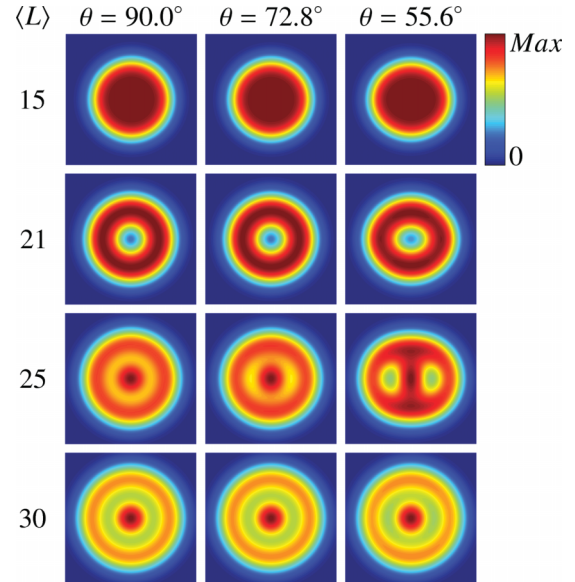

FIG. 2. (Color online) Probability densities for the states marked with circles in Fig. 1. The listed angular momentum values are approximate. Each subplot, here and in subsequent figures, is plotted in the intervals $-4 < x < 4$ (horizontally) and $-4 < y < 4$ (vertically). All plots are normalized to have the same peak height and plotted according to the shown color bar.

The density does not drop to zero at the vortex cores, but this typically does not happen in a finite-size system. For example, rotating bosons forming a single vortex exhibit zero density in the mean-field solution but have a nonzero density at the vortex core in the exact analytical solution for a specific finite number of particles [34–36].

C. Currents

While local minima in the density may indicate vortices, further support for their existence can be obtained by examining the probability current, as shown in Fig. 3. The current is here given as the expectation value of the operator (cf. Eqs. (3)– (5) in Ref. [33])

$$\hat{\mathbf{j}}(\mathbf{r}) = \sum_{i=1}^{N} \frac{-i}{2}[\delta(\mathbf{r} - \mathbf{r}_i)\nabla_i + \nabla_i\delta(\mathbf{r} - \mathbf{r}_i)] - (\Omega\mathbf{e}_z \times \mathbf{r})\hat{\rho}(\mathbf{r}),$$

(3)

where $\hat{\rho}(\mathbf{r}) = \sum_{i=1}^{N} \delta(\mathbf{r} - \mathbf{r}_i)$ and $\mathbf{e}_z$ is the unit vector of the z direction. The last term in the expression originates in the coordinate transformation we use here—the current (as all other calculated quantities) is given in the corotating reference frame. In principle one could obtain the velocity $\mathbf{v}$ by dividing the current with the density and then the vorticity as $\nabla \times \mathbf{v}$. However, in the regions where the density is very small this could yield numerically unstable results, and we here restrict ourselves to analyzing the more well-defined current.

For the two-vortex state discussed earlier, Fig. 3 shows the corresponding current, which can be seen to circulate around the density minima, supporting the interpretation of these minima as vortices. We note that in Fig. 3 the inner and outer regions of the system appear to be rotating in opposite
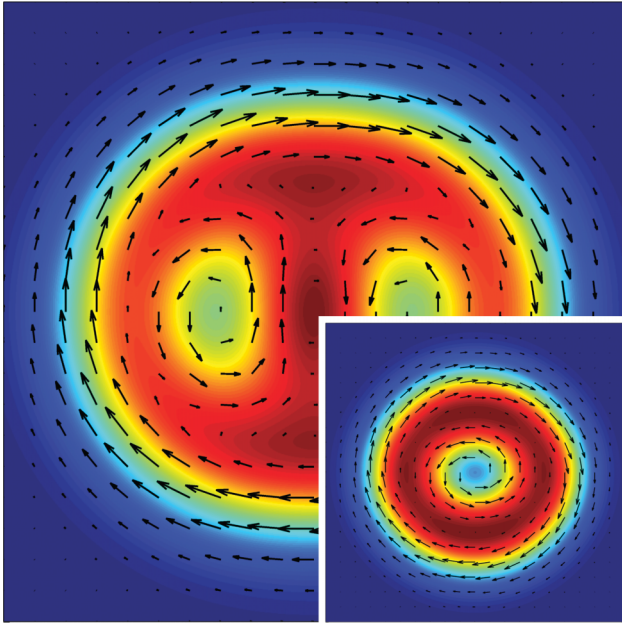
FIG. 3. (Color online) Probability current (as defined in the text) for the case $\langle L \rangle \approx 25$, when $\Theta = 55.6°$. The inset shows the case $\langle L \rangle \approx 21$, as a comparison. The black arrows show the current, on top of the single-particle density. In both cases shown, the current can be seen to loop around the density minima. As an effect of the calculations being performed in the corotating reference frame, the current in the outer parts of the particle cloud appear to rotate opposite to the current around the vortices. The same plotting conventions as in Fig. 2 are used here.

directions; this is, however, an effect of the corotating reference frame used here.

D. Pair-correlated densities

In Fig. 4 we show pair-correlated densities. Complementing the single-particle density, this quantity can give additional information about the internal structure of the state. The pair-correlated density is here defined as $\rho(\mathbf{r}, \mathbf{r}') = \langle \Psi | \hat{\Psi}^\dagger(\mathbf{r}) \hat{\Psi}^\dagger(\mathbf{r}') \hat{\Psi}(\mathbf{r}') \hat{\Psi}(\mathbf{r}) | \Psi \rangle$, giving the probability density of simultaneously finding two particles at positions $\mathbf{r}$ and $\mathbf{r}'$. In Fig. 5 we show pair-correlated densities for the state at $\Theta = 55.6°$ with a reference particle placed at different positions $\mathbf{r}'$, showing that the overall structure of the density is a stable configuration with two minima, although somewhat
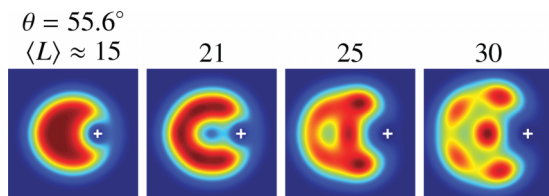

FIG. 4. (Color online) Pair-correlated densities for the states shown in the right column of Fig. 2, for which the dipole tilt angle is $\Theta = 55.6°$. The white cross marks the position of the reference particle. The same plotting conventions as in Fig. 2 are used here. The positions of the reference particle are here all on the x axis, and from left to right $x = 1.5$, 1.8, 2.3 and 2.4.
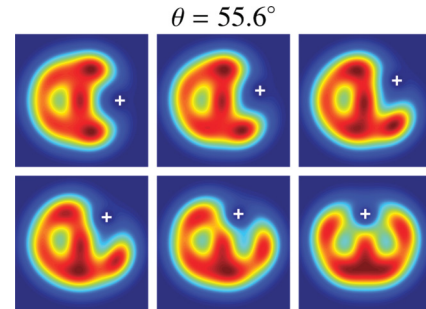

FIG. 5. (Color online) Pair-correlated densities for the state with $\langle L \rangle \approx 25$, for $\Theta = 55.6°$, with the reference particle placed at different positions (white crosses). Apart from the necessary fermionic exchange hole, the general structure of the state is not sensitive to the chosen position. The positions of the reference particle, starting from top left panel, were $(x, y) = (2.4, 0)$, $(2.2, 0.6)$, $(1.9, 1.2)$, $(1.5, 1.5)$, $(0.9, 1.7)$, and $(0, 1.7)$. The same plotting conventions as in Fig. 2 are used here.

obscured here by the so-called exchange hole around the position of the reference particle. (This effect is due to the Pauli exclusion principle, which implies that the probability to find any other particle must vanish near the position of the reference particle.)

For larger rotation, as Ω is increased further, the $N = 6$ system appears to have too few particles to support more vortices, and instead it undergoes a transition to a state where the particles are highly localized, as shown in Fig. 4. This is again very similar to the behavior of electrons in a strong magnetic field. Though not seen for the parameter regimes considered here, the anisotropic interaction can be expected to affect the geometries of such states (see Ref. [28]).

IV. SUMMARY

To summarize, we have shown that a quasi-two-dimensional trap with fermionic particles with dipole-dipole interactions show a response to induced rotation that is in many ways similar to that of confined electrons in a magnetic field [15]. This is perhaps naturally expected given that both appearing interactions in both cases are repulsive and long-ranged (as also discussed earlier in Refs. [26,27]). Here, however, we focused on the occurrence of vortices in repulsive fermion systems, which may show properties very similar to their superfluid cousins with bosons or attractive fermions. We found that a system of six dipolar fermions in a harmonic trap shows the characteristic stepwise increase of angular momentum as a function of the trap rotation. While the cloud first remains at rest, beyond a critical frequency the angular momentum shows a discontinuous jump by N units, and the first vortex penetrates the cloud. Additional vortices then occur with increasing Ω. We further analyzed how the vortices are affected by a tilt of the dipole axis. We find that although quantitatively the internal structure of the quantum state is in fact largely unchanged, the probability density of the two-vortex state is sensitive to the tilt angle, very clearly mapping out the internal symmetry of the quantum state. From a theoretical perspective, this yields a fortunate situation as it allows the broken symmetry of the state to be

analyzed directly via, for example, the density and current. For a rotationally symmetric Hamiltonian, this is typically not possible. In experiments, possibly any disorder or imperfection of the trap may already break the symmetry for aligned dipoles at $\theta = 90.0^\circ$.

In conclusion, our study suggests that there may be a possibility of experimentally observing vortices in a rotating quantum system without superfluidity, composed of spin-polarized fermions with repulsive dipole-dipole interactions.

[1] R. Donnelly, *Quantized Vortices in Helium II* (Cambridge University Press, Cambridge, 1991).

[2] S. Bose, Z. Phys. **26**, 178 (1924); A. Einstein, Sitz. ber. der Preuss. Akad. Wiss. 261 (1924); 3 (1925).

[3] M. Anderson, J. Ensher, M. Matthews, C. Wieman, and S. Cornell, Science **269**, 198 (1995); K. B. Davis, M. O. Mewes, M. A. Joffe, M. R. Andrews, and W. Ketterle, Phys. Rev. Lett. **74**, 5202 (1995); J. R. Ensher, D. S. Jin, M. R. Matthews, C. E. Wieman, and E. A. Cornell, *ibid.* **77**, 4984 (1996); E. Cornell and C. Wieman, Rev. Mod. Phys. **74**, 875 (2002); W. Ketterle, *ibid.* **74**, 1131 (2002).

[4] D. A. Butts and D. S. Rokshar, Nature (London) **397**, 329 (1999).

[5] G. M. Kavoulakis, B. Mottelson, and C. J. Pethick, Phys. Rev. A **62**, 063605 (2000).

[6] K. W. Madison, F. Chevy, W. Wohlleben, and J. Dalibard, Phys. Rev. Lett. **85**, 806 (2000).

[7] J. R. Abo-Shaer, C. Raman, J. M. Vogels, and W. Ketterle, Science **292**, 476 (2001).

[8] A. L. Fetter, Rev. Mod. Phys. **81**, 647 (2009).

[9] S. Giorgini, L. P. Pitaevskii, and S. Stringari, Rev. Mod. Phys. **80**, 1215 (2008).

[10] I. Bloch, J. Dalibard, and W. Zwerger, Rev. Mod. Phys. **80**, 885 (2008).

[11] S. M. Reimann and M. Manninen, Rev. Mod. Phys. **74**, 1283 (2002).

[12] H. Saarikoski, A. Harju, M. J. Puska, and R. M. Nieminen, Phys. Rev. Lett. **93**, 116802 (2004).

[13] M. Toreblad, M. Borgh, M. Koskinen, M. Manninen, and S. M. Reimann, Phys. Rev. Lett. **93**, 090407 (2004).

[14] S. Viefers, J. Phys.: Condens. Matter **20**, 123202 (2008).

[15] H. Saarikoski, S. M. Reimann, A. Harju, and M. Manninen, Rev. Mod. Phys. **82**, 2785 (2010).

[16] H. Saarikoski and A. Harju, Phys. Rev. Lett. **94**, 246803 (2005).

[17] F. Serwane, G. Zurn, T. Lompe, T. B. Ottenstein, A. N. Wenz, and S. Jochim, Science **332**, 6027 (2011).

[18] T. Koch, T. Lahaye, J. Metz, B. Frölich, A. Griesmaier, and T. Pfau, Nat. Phys. **4**, 218 (2008).

[19] M. Lu, S. H. Youn, and B. L. Lev, Phys. Rev. Lett. **104**, 063001 (2010).

[20] J. G. Danzl, M. J. Mark, E. Haller, M. Gustavsson, R. Hart, J. Aldegunde, J. M. Hutson, and H.-C. Nägerl, Nat. Phys. **6**, 265 (2010).

[21] J. Deiglmayr, A. Grochola, M. Repp, K. Mörtlbauer, C. Glück, J. Lange, O. Dulieu, R. Wester, and M. Weidemüller, Phys. Rev. Lett. **101**, 133004 (2008).

[22] S. Müller, J. Billy, E. A. L. Henn, H. Kadau, A. Griesmaier, M. Jona-Lasinio, L. Santos, and T. Pfau, Phys. Rev. A **84**, 053601 (2011).

[23] C. Trefzger, C. Menotti, B. Capogrosso-Sansone, and M. Lewenstein, J. Phys. B **44**, 193001 (2011).

[24] T. Lahaye, C. Menotti, L. Santos, M. Lewenstein, and T. Pfau, Rep. Prog. Phys. **72**, 126401 (2009).

[25] M. A. Baranov, Phys. Rep. **464**, 71 (2008).

[26] K. Osterloh, N. Barberán, and M. Lewenstein, Phys. Rev. Lett. **99**, 160403 (2007).

[27] M. A. Baranov, H. Fehrmann, and M. Lewenstein, Phys. Rev. Lett. **100**, 200402 (2008).

[28] R.-Z. Qiu, S.-P. Kou, Z.-X. Hu, X. Wan, and S. Yi, Phys. Rev. A **83**, 063633 (2011).

[29] J. C. Cremon, G. M. Bruun, and S. M. Reimann, Phys. Rev. Lett. **105**, 255301 (2010).

[30] S. Yi and H. Pu, Phys. Rev. A **73**, 061602(R) (2006).

[31] S. Komineas and N. R. Cooper, Phys. Rev. A **75**, 023623 (2007).

[32] Y. Cai, M. Rosenkranz, Z. Lei, and W. Bao, Phys. Rev. A **82**, 043623 (2010).

[33] H. Saarikoski, S. M. Reimann, E. Räsänen, A. Harju, and M. J. Puska, Phys. Rev. B **71**, 035421 (2005).

[34] N. K. Wilkin, J. M. F. Gunn, and R. A. Smith, Phys. Rev. Lett. **80**, 2265 (1998).

[35] G. F. Bertsch and T. Papenbrock, Phys. Rev. Lett. **83**, 5412 (1999).

[36] B. Mottelson, Phys. Rev. Lett. **83**, 2695 (1999).